3rd IEEE International Conference on Sensors, Vienna, Austria, October 24-27, 2004

Reliability Evaluation of Direct Chip Attached Silicon Carbide Pressure Transducers

Robert S. Okojie[1], Ender Savrun[2], Phong Nguyen[2],Vu Nguyen[2], and Charles Blaha[3]
[1]NASA Glenn Research Center, Cleveland, OH, USA, robert.s.okojie@nasa.gov
[2]Sienna Technologies, Inc., Woodinville, WA, USA, ender.savrun@siennatech.com
[3]Akima Corporation, Fairview, OH, USA, charles.a.blaha@grc.nasa.gov

Abstract
An accelerated stress test (AST) protocol has been developed and used to evaluate the reliability of 6H-silicon carbide (SiC) pressure transducers for operation up to 400 °C for 100 hours. After several cyclic excursions to 400 °C, the maximum drift of the zero pressure offset voltage at 25 °C was 1.9 mV, while the maximum drift at 400 °C was 2.0 mV. The full-scale sensitivity to pressure before and after the AST was 36.6 μV/V/psi at 25 °C and 20.5 μV/V/psi at 400 °C, with a maximum drift of ± 1 μV/V/psi. No systematic degradation of the zero pressure offset was observed.

Keywords
Silicon carbide, High Temperature, Pressure Sensor, Package, Reliability.

INTRODUCTION
Pressure monitoring during deep well drilling and in automobiles and jet engines requires pressure sensors and electronics that can operate reliably at temperatures between 200 °C and 600 ºC [1, 2]. Conventional silicon semiconductor pressure transducers increasingly suffer from instability and failure as the operation is extended to the higher end of the above temperature range. The reasons include degradation of metal/semiconductor electrical contacts and weakening of bond wires due to temperature-driven intermetallic diffusion [3]. In order to extend the silicon pressure sensor operating temperature, several commercial pressure transducers employ complex and costly packaging schemes (e.g., water cooling) to help maintain reliable and accurate operation. However, the complexity and cost disadvantages of such schemes are compounded by increase in weight, volume, and additional connections.

Silicon Carbide (SiC) semiconductor electronics and sensors have been demonstrated to operate at temperatures up to 600 °C [4,5]. Recently, Masheeb *et al.* reported the demonstration of a leadless (no wire bond) SiC-based pressure transducer at 500 °C [6]. The elimination of the gold bonds and the protection of the metallization from the harsh environment offer the potential for long-term survival of SiC pressure transducers at high temperature. These developments have increased the possibility of direct insertion of un-cooled SiC pressure sensors into high temperature environments. However, for SiC pressure sensor technology to transition from the laboratory to commercial production, several reliability challenges, including package-induced stress and contact degradation, must be resolved. To be commercially viable, these sensors must undergo appropriate reliability testing standards that are specific for harsh environment microsystems. The existing Joint Electron Device Engineering Council reliability testing standards are only applicable to conventional-environment semiconductor microsystems [7]. Because of the absence of a testing standard for high temperature devices, we had previously developed and employed an Accelerated Stress Testing (AST) protocol to evaluate the reliability performance of packaged SiC pressure transducers up to 300 °C in air for over 140 hours under cyclic pressure and temperature [8]. In this work, a revised and more demanding AST protocol was used to evaluate the pressure transducer reliability up to 400 °C.

Reliability by package design
The SiC sensor die (2.1x2.1 mm^2)is mounted on an aluminum nitride (AlN) header (0.25 in. diameter) by the direct chip attach (DCA) method, as shown in Fig. 1, so that only the sensor's circular diaphragm is free to deflect in and out of the reference cavity [9]. The sealing glass is applied only into and above the narrow gap (< 10 μm) between the SiC sensor and the inner walls of the AlN, thereby providing a reference pressure in the cavity. This DCA approach eliminates the need for wirebonding, thereby eliminating failure mechanisms associated with high temperature diffusion of gold bond wires [3]. Because the sealing glass is applied at T_δ = 750 °C, the SiC/glass interface is assumed to be in a relaxed stress-free state. Upon cooling to room temperature, the mismatches in the coefficients of thermal expansion (CTE) of the contracting components induce a net stress on the SiC sensor. This package-induced stress is a primary cause of transducer instabilities during cyclic temperature excursions and must be significantly minimized. Therefore, having components with equal CTE's will ideally eliminate the package-induced stress. AlN is selected because its CTE (α_{AlN} = 4.1 ppm/°C) is close to that of SiC (α_{SiC} = 3.7 ppm/°C). The CTE of the sealing glass (~4.1 ppm/°C) is also close to that of SiC. Thus, the resulting induced net strain on the SiC sensor as a result of the packaging process can be estimated as:

$$\varepsilon_\delta = (\alpha_{glass} - \alpha_{SiC})(T_\delta - T) \quad (1)$$

This contributes a lateral residual strain of about 300 μstrains on the SiC sensor contact solid surface at room temperature. The greater than 12 mm distance separating the SiC sensor and the kovar tube (Fig. 1) ensures that the large thermomechanical stress between the kovar and AlN does not propagate to the SiC sensor [8].

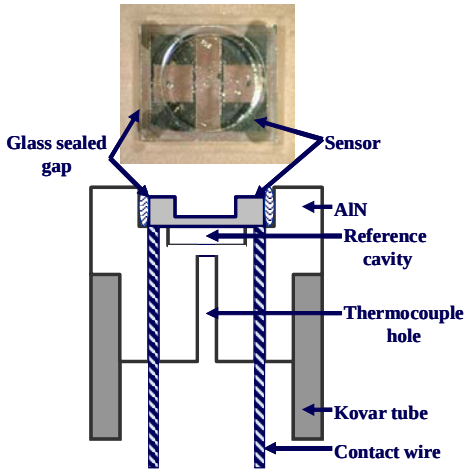

Figure 1: Top and cross-sectional views of MEMS-DCA package featuring direct wire contact to sensor and thermocouple access hole for temperature compensation, and calibration.

Transducer parametric analysis

The resistors are arranged in a Wheatstone bridge configuration shown in Fig. 2, which ideally will have a pressure offset voltage, $V_{oz,}$ of zero if all resistors are exactly the same. Deviation from perfect resistor symmetry results in a non-zero V_{oz} across the bridge that is expressed as:

$$V_{oz} = \frac{V_{in}}{2}\left(\frac{R_2 - R_1}{R_1 + R_2} + \frac{R_4 - R_3}{R_3 + R_4}\right) \quad (2)$$

where $R_{1,}$ R_2, R_3, and R_4 are the bridge resistor elements (Ω) and V_{in} is the input voltage (V). Another influence on V_{oz} is the thermomechanical package-induced stress discussed above. The relative change in each resistor element due to externally applied and residual strain is generally expressed as:

$$\Delta R = R(\varepsilon + \varepsilon_\delta)G \quad (3)$$

where G represents the gauge factor (strain sensitivity factor) of the resistor element, and ε is the strain resulting from the applied pressure. The temperature coefficient of resistance (TCR) of a resistor, denoted as β (ppm/°C), approximates the resistor value via the expression:

$$R(T) = R_o(1 + \beta\Delta T) \quad (4)$$

where R_o is the resistance at the reference temperature (room temperature), and ΔT (°C) is the temperature change from the reference temperature. The temperature effect of the gauge factor is similarly modeled by:

$$G(T) = G_o(1 + \gamma\Delta T) \quad (5)$$

where γ is the temperature coefficient of gauge factor (TCGF) (ppm/°C) and G_o is the gauge factor at the reference temperature. It is important to note that under an unstrained condition (i.e., no applied pressure and sensor not packaged), the bridge output is governed only by equations (2) and (4). With the sensor attached to the package at elevated temperature and cooled down to room temperature, it experiences a package-induced residual strain, as expressed in equation (1), thus creating a change in the resistance and V_{oz}. When pressure and temperature are applied simultaneously, each resistor element experiences a relative change expressed by combining equations (1) and (3-5) as:

$$\Delta R(T) = R_o G_o\left[1 + (\beta + \gamma)\Delta T + \gamma\beta(\Delta T)^2\right](\varepsilon + \varepsilon_\delta) \quad (6)$$

Therefore, with the sensor fully packaged and no applied pressure (ε=0), the change in resistance with temperature results in change in V_{oz}. As the operating temperature increases, ε_δ will decrease correspondingly (relaxation) and the resistance change becomes largely governed by β and less by γ parameters. Equation (6) is particularly important for understanding the overall behavior of the transducer, especially with regard to temperature compensation and transducer calibration. It also reveals the effect of thermomechanically-induced stress on the system and its deleterious effect on the long-term output stability.

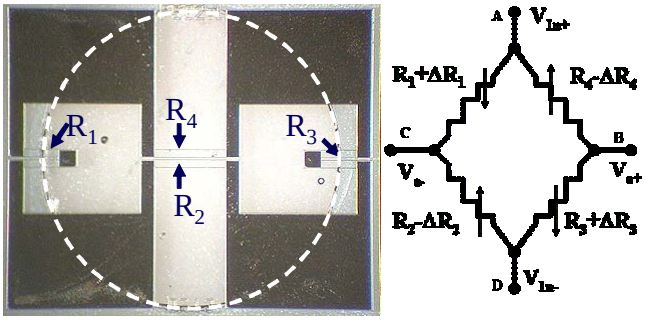

Figure 2: Scanning electron micrograph (top view) of a 6H-SiC pressure sensor showing the four resistors and the outline of the circular backside diaphragm. The bridge equivalent circuit diagram is on the right.

AST protocol

The AST protocol used is shown in Fig. 3. We evaluated the stability and reliability of 6H-SiC pressure transducers at temperatures starting from 25 °C up to the temperature of instability onset, $T_{unstable,}$ This is the temperature at which the V_{oz} fluctuates such that no reliable pressure measurement can be performed. The initial pressure tests at room temperature are performed in Step 1 where twenty cycles of *0* psi $\rightarrow P_{max} \rightarrow$ *0* psi are applied at steps of 10%P_{max} and held for ten seconds per step. The pressure, P_{max}, was pre-determined to be 100 psi from previously validated finite element modeling and burst pressure analysis. The failing transducers after this step are removed for failure analysis (FA) to determine the failure mechanisms. The passing transducers after Step 1 are thus validated to handle the maximum pressure. In Step 2, the

transducers were heated from room temperature to 100 °C and cycled 20 times between 0 psi and 100 psi. This 20-cycle pressurization is repeated at increments of 100 °C following 1-hour zero pressure stabilization at each temperature increment.

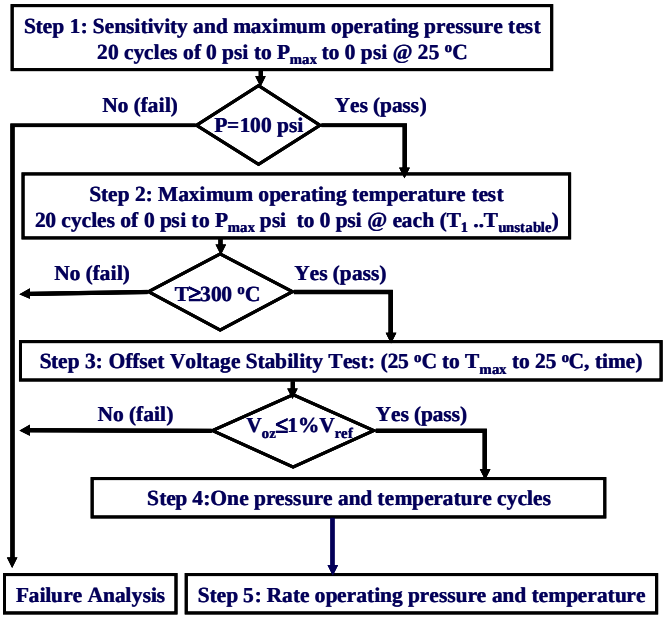

Figure 3: The AST protocol for evaluating the long term reliability of SiC pressure sensors at high temperature.

This intermittent procedure continues at every temperature until instability is observed at $T_{unstable}$. Thus, Step 2 ascertains the maximum temperature T_{max} at which the V_{oz} remains stable. Devices that exhibit instability in Step 2 at temperatures below 300 °C are screened out. The transducers that exhibit $T_{max} \geq 300$ °C proceed to Step 3, where they are subjected to their corresponding T_{max} as function of time. Prior to the start of Step 3, the room temperature reference offset voltage, V_{ozref} (25 °C) and the V_{ozref} (T_{max}) are recorded. From then on the offset voltage values at the two temperatures (25 °C and T_{max}) are recorded after each cycle of heating and cooling over time. The dwell time at T_{max} is arbitrarily chosen. The deviations of zero pressure offset voltages from the V_{ozref} values at these two temperature extremes determine the degree of stability of the transducer. Finally, in Step 4, another round of pressurization and temperature treatment (one cycle of pressure and temperature ramp up and ramp down) is performed on the passing transducers to rate operating sensitivity, pressure, and temperature.

Stability of transducer parameters

Only six of the twelve 6H-SiC transducers evaluated survived to Step 4 of the AST. The results of the failure analyses on the failed transducers will be subject of a future publication. For the passing transducers, three were evaluated at T_{max} of 300 °C while the other three were evaluated at 400 °C. The $V_{oz}(T)$ of a representative transducer from the 400 °C batch is shown in Fig. 4a, as recorded during the last cool down sequence at the end of Step 3 of the AST protocol. It shows the V_{oz} (P=0, T), for an applied bridge input voltage V_{in} = 5 V. The plot of the full-scale (100 psi) response as function of temperature is also included to show the dynamic operating range of the transducer and the effect of temperature. From the plots, the functional difference between the V_{oz}(P=0 psi, T) and V_o(P=100 psi, T) becomes slightly smaller with increasing temperature. This is shown from different perspectives in Figs. 4b and 4c in terms of the dynamic range (net bridge output) and strain sensitivity as function of pressure at various temperatures, which show the characteristic drop in net pressure, net output voltage, strain and sensitivity with increasing temperature, respectively. This behavior is characteristic of piezoresistive sensors [4, 6]. The strain sensitivity at 400 °C as plotted in Fig. 4c shows it still retains about 60% of its room temperature value. Although

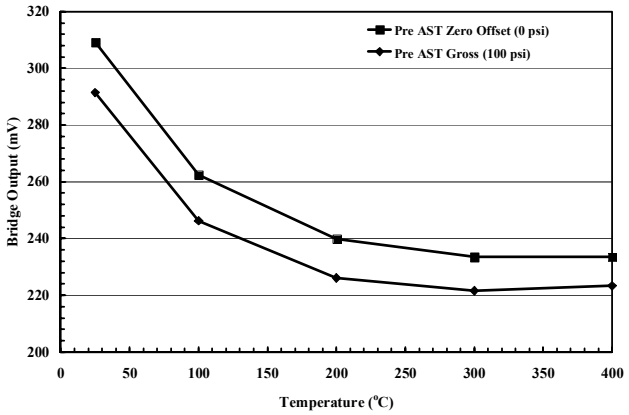

Figure 4a: Zero offset of one sensor during final cool down sequence at the end of Step 3 of the AST protocol. Also shown is the full-scale output at 100 psi.

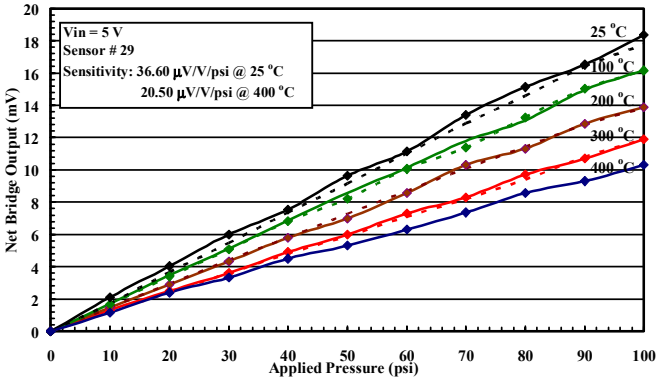

Figure 4b: Net voltage after Step 4. Solid and dashed plots represent heating and cooling excursions, respectively.

not shown, the drift in the full-scale sensitivity as function of time at the two temperature extremes remains within ± 1 µV/V/psi of the reference values, which is equivalent to errors of 2.9% and 4.8% at 25 °C and 400 °C, respectively.

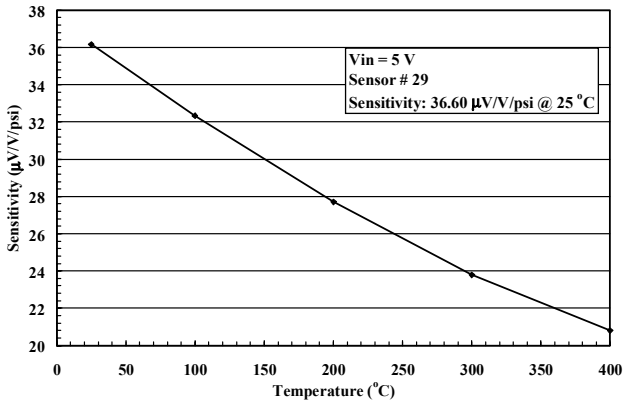

Figure 4c: Effect of temperature on the strain sensitivity after Step 4 of the AST.

Long Term Stability

The long-term stability of the transducer V_{oz} during Step 3 was evaluated by cyclic heating and cooling of the two batches separately from 25 °C to their respective T_{max} (Step 3) over time. For the T_{max} = 300 °C sub-batch, Fig. 5a shows that after 145 hours the maximum drift of V_{oz} (25 °C, t) from

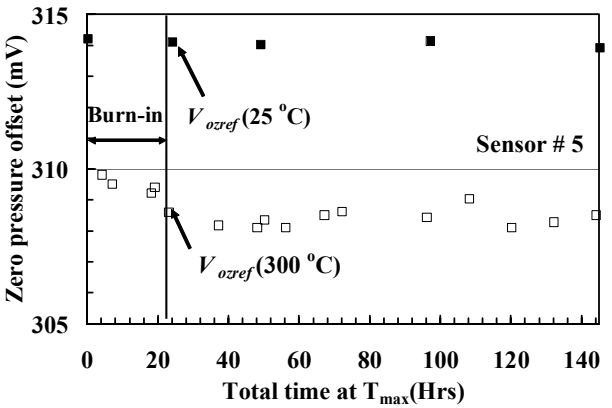

Figure 5a: Time history of zero offset of a 300 °C device after 145 hours of cyclic heating at 300 °C and cooling.

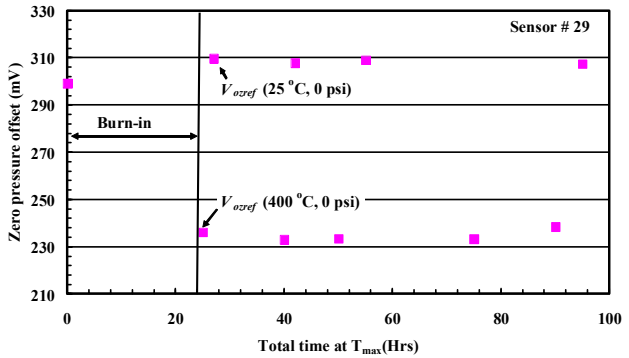

Figure 5b: Zero pressure offset from a 400 °C device after 90 hours of cyclic heat heating to 400 °C and cooling to room temperature.

V_{ozref} (25°C) is 0.5 mV. Similarly, the maximum drift in V_{oz} (300 °C, t) was approximately 0.6 mV from V_{ozref} (300°C). With regard to the 400°C sub-batch, the maximum drifts of V_{oz} (25°C, t) and V_{oz} (400°C, t) from their corresponding references were 1.9 mV and 2.0 mV, respectively. In both cases, the reference values are set after a 24-hr transducer burn-in period. In both sub-batches, the drifts in the V_{oz} are observed to fluctuate around the reference values, as opposed to irreversible degradation of the transducer.

CONCLUSION

We have developed a refined AST protocol and used it screen and evaluate the reliability of MEMS-DCA packaged SiC pressure transducers that operated reliably at 400 °C over 100 hours. This AST protocol can be used as an initial tool in developing a better understanding and measure long-term performance characteristics of SiC pressure transducers, thus making it possible to have an effective and accurate calibration scheme. Effort is currently underway to use this protocol to evaluate transducers beyond 400°C.

ACKNOWLEDGEMENTS

This work was funded under the Technology Transfer Project at NASA Glenn Research Center. We wish to thank the technical staff of the SiC Microsystems Fabrication Laboratory at NASA-Glenn for fabrication, sample preparation, and metrology.

REFERENCES

[1] Alexandar's Gas and Oil Connections, News and Trends: North America, vol. 8 Issue 13. (2003).

[2] L. G. Matus, J.A. Powell, and C.S. Salupo, "High-voltage 6H-SiC p-n junction diodes", Appl. Phys. Lett., vol. 59, pp 1770-1772, (1991).

[3] M. Khan, H. Fatemi, J. Romero, and E. Delenia, "Effect of high thermal stability mold material on the gold-aluminum bond reliability in epoxy encapsulated VLSI devices," Proc. 26th International Reliability Physics Symposium, April, 12-14, pp. 40-49. (1988)

[4] R. S. Okojie, "Characterization of 6H-SiC as a Piezoresistive Pressure Sensor for High Temperature Applications," Ph. D. Thesis, New Jersey Institute of Technology, Newark, NJ. (1996).

[5] P. G. Neudeck, R. S. Okojie, and L. -Yu Chen, "High-temperature electronics-a role for wide bandgap semiconductors? Proc. IEEE, Vol. 90, Issue 6, pp. 1065–1076, (2002).

[6] F. Masheeb, S. Stefanescu, A. A. Ned, A. D. Kurtz, and G. Beheim, "Leadless sensor packaging for high temperature applications," The 5th IEEE Intl. Conf. Micro Electro Mechanical, pp. 392–395, Jan. 2002.

[7] See http:www.jedec.org for applicable standards.

[8] E. Savrun, V. Nguyen, and R. S. Okojie, "A Silicon Carbide Pressure Sensor for High Temperature (600ºC) Applications," IMAPS International High Temperature Electronics Conference, Santa Fe, NM, May 17-20, (2004).

[9] Robert S. Okojie, "MEMS Direct Chip Attach (MEMS-DCA) Packaging Methodologies for Harsh Environments", Patent pending.